Available online at www.sciencedirect.com

ScienceDirect

IFAC Papers Online CONFERENCE PAPER ARCHIVE

IFAC PapersOnLine 53-2 (2020) 8605–8612

# Fractional-order Control: Nyquist Constrained Optimization

**Andreas H. Moltumyr** * **Michael R.P. Ragazzon** *
**Jan T. Gravdahl** *

* *Department of Engineering Cybernetics, NTNU, Norwegian University of Science and Technology, Trondheim, Norway (e-mail: {andreas.h.moltumyr, michael.remo.ragazzon, jan.tommy.gravdahl}@ntnu.no)*

**Abstract:** The adoption of fractional calculus in control systems has enabled the synthesis of new controllers with fractional-order derivatives and integrals. Several optimization-based methods for tuning of linear fractional-order controllers have been explored. However, few have considered the stability of the closed-loop system during optimization. This paper presents a model-driven method for tuning of fractional-order controllers based on a heuristic optimization technique and the experimental use of Nyquist's stability criterion to enforce closed-loop stability of fractional-order systems. The proposed frequency domain tuning method enables tuning of linear fractional-order controllers with few to medium number of parameters. The method can handle both fractional-order linear and integer-order linear plant models and controllers. To assist the experimental use of Nyquist's stability criterion, a function for drawing a Logarithmic amplitude polar diagram has been developed. Simulation results of the method applied to a nanopositioning system in atomic force microscopy suggest that the proposed method can be used for optimization of fractional-order controllers while enforcing closed-loop stability. Given that the system can be stabilized with the given controller. Matlab code building on the FOTF toolbox and global optimization toolbox is provided.



*Keywords:* Micro and Nano Mechatronic Systems, Fractional systems, Fractional-order control, Nyquist's criterion, Genetic algorithms, Logarithmic Nyquist diagram.

## 1. INTRODUCTION

The topic of fractional-order calculus for control has received increased attention in recent years, however, the mathematical foundation of fractional-order calculus was laid out in the nineteenth century (David et al., 2011). Fractional-order or irrational-order differentiation is a generalization of integer-order differentiation from the set of natural to the set of real numbers.

Several papers on fractional-order control reports on increased performance. However, most of these results show only minor improvements when compared to well established integer-order controllers. Dastjerdi et al. (2018) proposed rules of thumb for tuning of fractional-order PID controllers. Dabiri et al. (2018) tuned a set of variable-order fractional PID controllers using the particle swarm optimization (PSO) algorithm. Mandić et al. (2017) used dominant pole placement and the D-decomposition approach in tuning a fractional-order PID controller. Sun et al. (2018) proposed a fractional-order sliding mode controller for tracking control of a linear motor. Kumar et al. (2018) tuned a fractional-order PID controller using an evolutionary multi-objective optimization algorithm. Guefrachi et al. (2017) proposed a fractional-complex-order PID controller. Altintas and Aydin (2017) compared the use of the Big Bang Big Crunch optimization algorithm and the genetic algorithm in tuning fractional-order and integer-order PID controllers for a MAGLEV system.

Stability analysis and stability of closed-loop systems are important when designing and tuning feedback controllers. In the literature, Matignon's stability theorem is dominating (Matignon, 1996). However, this stability analysis method quickly turns infeasible for large fractional-order transfer functions or low commensurate-orders because of high computational complexity of calculating the roots. A few other stability analysis techniques for fractional-order systems are mentioned in (Sabatier et al., 2013).

Nyquist's stability criterion has been used extensively for stability analysis of closed-loop systems in the case of integer-order linear time-invariant (LTI) systems and is usually taught in basic control theory courses on frequency domain techniques. However, the use of this criterion for fractional-order systems has not been studied extensively in the literature. Trigeassou and Maamri (2009) considered the use of Nyquist criterion for stability analysis of fractional differential equations and included systems with time delays in the study. Similarly, Zhou (2017) considered a Nyquist-like criterion for fractional-order linear time-invariant differential equations and examined necessary and sufficient conditions in addition to the choice of integral contour for applying the argument principle. Trächtler (2016) considered BIBO stability of a class of irrational transfer functions and proposed a generalization of the Nyquist criterion, focusing on poles, zeros and Riemann surface branch points. Xue (2017) also comments that: "In


10.1016/j.ifacol.2020.12.519

the original Nyquist theorem, there was no assumption that $G(s)$ is a rational integer-order transfer function. Therefore, the theorem should be valid for fractional-order, or even, irrational systems."

In this paper, a method for tuning of fractional-order controllers is presented. The method uses the genetic algorithm for controller parameter tuning, a heuristic optimization technique. To enforce stability of the optimized solution, a constraint that automatically evaluates the Nyquist stability criterion has been added to the optimization problem. A custom adaptive frequency stepping algorithm for fast frequency response calculation has been developed to make the evaluation of the Nyquist criterion effective. Simulations reveal that the presented tuning method enables tuning of a wide set of fractional-order linear controllers with arbitrary structure as opposed to many of the fractional-order controller tuning methods proposed in the literature, of which most focus on the fractional-order PID controller. Simulations with Simulink and the FOTF toolbox (Xue, 2017), building on the Oustaloup fractional-order realization technique (Oustaloup et al., 2000), reveal that the calculated gain margins reported from the automatic stability assessment are correct.

To the authors' best knowledge, the Nyquist criterion has never been used as a constraint in optimization-based tuning in the proposed way and in particular not in the context of fractional-order control systems. Matlab code is provided (Moltumyr, 2019a).

## 2. PRELIMINARIES

### *2.1 Fractional-order systems*

Fractional-order control systems build on fractional calculus which generalizes integer-order derivatives and integrals to arbitrary order derivatives and integrals. There exist many different definitions of fractional derivatives and integrals. One of the most used definitions is the Riemann-Liouville definition (Podlubny, 1999).

The Riemann-Liouville definition for a fractional derivative (Podlubny, 1999), given $\alpha > 0$ and $n = \lceil \alpha \rceil$, is

$$ {}_{x_0}\mathcal{D}_x^{\alpha} f(x) = \frac{1}{\Gamma(n-\alpha)} \frac{\mathrm{d}^n}{\mathrm{d}x^n} \int_x^{x_0} \frac{f(\tau)}{(x-\tau)^{1+\alpha-n}} \mathrm{d}\tau, \quad (1) $$

where $\Gamma(\cdot)$ is the gamma function. The Riemann-Liouville definition of a fractional integral (Xue, 2017) is

$$ {}_{x_0}\mathcal{D}_x^{-\alpha} f(x) = \frac{1}{\Gamma(\alpha)} \int_x^{x_0} \frac{f(\tau)}{(x-\tau)^{1-\alpha}} \mathrm{d}\tau. \quad (2) $$

The Laplace transformation of a Riemann-Liouville fractional derivative (1) is

$$ \mathcal{L}\left\{\mathcal{D}_t^{\alpha} f(t)\right\}(s) = s^{\alpha} F(s) - \sum_{k=0}^{(\lceil \alpha \rceil - 1)} s^k \, \mathcal{D}_t^{(\alpha-k-1)} f(t)\Big|_{t=0}. \quad (3) $$

This motivates the use of Laplace domain and frequency domain methods and expressions when designing linear fractional-order control systems.

Based on (3), a general fractional-order transfer function with input $u(s)$ and output $y(s)$ can be expressed as

$$ \frac{y(s)}{u(s)} = \frac{b_m s^{\gamma_m} + b_{m-1} s^{\gamma_{m-1}} + \ldots + b_1 s^{\gamma_1} + b_0 s^{\gamma_0}}{a_n s^{\eta_n} + a_{n-1} s^{\eta_{n-1}} + \ldots + a_1 s^{\eta_1} + a_0 s^{\eta_0}}, \quad (4) $$

where $m$ and $n$ are the numbers of different fractional-order parts in numerator and denominator, respectively. $\gamma_l$ and $b_l$ are the corresponding fractional orders and coefficients of the numerator, while $\eta_i$ and $a_i$ are the corresponding fractional orders and coefficients of the denominator. Without loss of generality we assume that $0 \leq \eta_i < \eta_{i+1}$ and $0 \leq \gamma_l < \gamma_{l+1}$.

In the following, we will use $C(s)$ to denote a controller transfer function, $G(s)$ to denote a plant transfer function,

$$ L(s) = C(s)G(s), \quad (5) $$

for an open-loop system, and

$$ T(s) = \frac{L(s)}{1 + L(s)}, \quad (6) $$

for a closed-loop system (complementary sensitivity function).

$$ S(s) = \frac{1}{1 + L(s)}, \quad (7) $$

is the sensitivity function.

### *2.2 Oustaloup Filter Approximation*

Fractional-order integrals and derivatives, as opposed to integer-order integrals and derivatives, are problematic to realize with digital computers because of the infinite memory effect (Dorćák et al., 2002). However, several approximation techniques have been developed (Xue, 2017). One of the most prominent approximation techniques is the Oustaloup filter approximation technique (Oustaloup et al., 2000), where a fractional-order derivative $s^{\alpha}$ is approximated in the frequency domain by several integer-order pole-zero pairs. This realization technique is used for simulation purposes in this paper through the usage of Simulink and the FOTF toolbox (Xue, 2017).

The integer-order filter approximation is formulated as:

$$ s^{\alpha} \approx K \prod_{k=1}^{N} \frac{s + \omega_k'}{s + \omega_k}, \quad (8) $$

$$ \omega_k' = \omega_b \, \omega_u^{(2k-1-\alpha)/N}, \qquad K = \omega_h^{\alpha}, \quad (9) $$

$$ \omega_k = \omega_b \, \omega_u^{(2k-1+\alpha)/N}, \qquad \omega_u = \sqrt{\frac{\omega_h}{\omega_b}}. \quad (10) $$

where $\alpha$ is the fractional-order, $\omega_b$ and $\omega_h$ is the lower and upper bound of the frequency area of interest where the approximation is valid, and $N$ is the number of pole-zero pairs, also called the order of the filter.

### *2.3 Nyquist's stability criterion*

Nyquist's stability criterion (Nyquist, 1932) is extensively used for analysing stability of closed-loop integer-order linear systems. In the proposed method, we use this

criterion to ensure closed-loop stability of the solution, as proposed for fractional-order systems by Xue (2017).

Nyquist's stability criterion states that an open-loop system $L(s)$ will be closed-loop stable iff

$$\Delta\angle\left(1+L(s)\right) = -2\pi\left(N_n - N_p\right), \tag{11}$$

where $\Delta\angle(1+L(s))$ is the sum of the argument of $1+L(s)$ when integrated along a closed-loop path enclosing the whole of the right half complex plane, and $N_n$ and $N_p$ are the number of right half plane zeros and right half plane poles in the transfer function $1+L(s)$, respectively.

A stable closed-loop system is usually desired. This is equivalent to setting $N_n = 0$. This leads to the simpler form $\Delta\angle(1+L(s)) = 2\pi N_p$, with the following interpretation: The number of counter-clockwise rotations of $\angle(1+L(s))$ must equal the number of right half plane poles for the open-loop system $N_p$, in order for the closed-loop system to be stable.

## 3. PROPOSED TUNING METHOD

A method for tuning fractional-order controllers with few parameters has been developed. The method is based on constrained optimization in the frequency domain, where the genetic algorithm (GA) (Holland, 1992) is combined with an algorithm developed in this work for the automatic calculation of Nyquist's stability criterion. The genetic algorithm implementation from the global optimization toolbox (MathWorks, 2019) has been used. See Moltumyr (2019a) for GA implementation choices. In this paper, the letter $j$ will be used for the imaginary unit.

### *3.1 Optimization Problem*

The method heuristically solves the following non-linear constrained and linearly bounded minimization problem:

$$\min_{\boldsymbol{x}} f(\boldsymbol{x}) \quad \text{s.t.} \begin{cases} c_1(\boldsymbol{x}) \leq 0, \\ c_2(\boldsymbol{x}) \leq 0, \\ \boldsymbol{x}_{lower} \leq \boldsymbol{x} \leq \boldsymbol{x}_{upper}, \end{cases} \tag{12}$$

where $f(\boldsymbol{x})$ is the objectivity function to be minimized, $\boldsymbol{x}$ are the controller parameters and the constraint functions used to ensure stability are

$$c_1(\boldsymbol{x}) = \Delta k - \mathrm{GM}_{\mathrm{high}} \leq 0, \tag{13}$$
$$c_2(\boldsymbol{x}) = \mathrm{GM}_{\mathrm{low}} + \Delta k \leq 0. \tag{14}$$

$\mathrm{GM}_{\mathrm{high}}$ and $\mathrm{GM}_{\mathrm{low}}$ are the gain margins, in decibel, that would place the system at the upper and lower stability boundaries of the closest stable area if such an area exists. Furthermore, $\Delta k$ is a gain margin parameter that can be set in order to ensure that the system will have a minimum gain margin $\Delta k$ dB, if possible.

In order for the closed loop response to be fast and not show excessive oscillations, $f(\boldsymbol{x})$ has been chosen to maximize system bandwidth $\omega_{bw}$, while keeping $|T(j\omega)|$ close to 0 dB for $\omega < \omega_{bw}$ and $|S(j\omega)|$ close to 0 dB for $\omega > \omega_{bw}$ (Skogestad and Postlethwaite, 2001). Building on (Eielsen et al., 2014), $f(\boldsymbol{x})$ was defined as

$$f(\boldsymbol{x}) = \gamma_1 f_1(\boldsymbol{x}) + \gamma_2 f_2(\boldsymbol{x}) + \gamma_3 f_3(\boldsymbol{x}), \tag{15}$$
$$f_1(\boldsymbol{x}) = \frac{1}{N_{bw}} \left( \sum_{i=0}^{N_{bw}} \left(1 - |T(j\omega_i;\boldsymbol{x})|\right)^2 \right)^{\frac{1}{2}}, \tag{16}$$
$$f_2(\boldsymbol{x}) = \frac{1}{N - N_{bw}} \left( \sum_{i=N_{bw}}^{N} \left(1 - |S(j\omega_i;\boldsymbol{x})|\right)^2 \right)^{\frac{1}{2}}, \tag{17}$$
$$f_3(\boldsymbol{x}) = -\omega_{bw} = -\omega_{N_{bw}(\boldsymbol{x})}, \tag{18}$$

Here, $\gamma_1$, $\gamma_2$, $\gamma_3 > 0$ are used to weigh the different objectives. $\omega_i$ for $i = 0, 1, \cdots, N_{bw}, \cdots, N$ are logarithmically spaced frequencies in the area where the objective should be calculated. $N$ is the total number of frequency values and $N_{bw}(\boldsymbol{x})$ is the index of the frequency vector where the bandwidth is found.

The objectives can be summarized as follows:

- $f_1$ Flatness of complementary sensitivity function $T(s)$ up to the defined bandwidth (How well $T(s)$ follows the 0-dB line).
- $f_2$ Flatness of sensitivity function $S(s)$ after the defined bandwidth (How well $S(s)$ follows the 0-dB line).
- $f_3$ High bandwidth, $\omega_{bw}$ (defined as the minimum of the first time $T(s)$ drops below $-6$dB and the first time $S(s)$ rises above $-6$dB).

The proposed objectivity function and the minimization problem is non-convex. Therefore, several local minima exist and a set of globally optimal controller parameters can not be guaranteed. However, the use of a random seeded population-based optimization method like the genetic algorithm enables the optimization to escape local minima if an individual of the population has found a better set of controller parameters.

### *3.2 Automatic calculation of Nyquist stability criterion*

Using Nyquist's stability criterion in optimization to ensure stability requires an automatic evaluation of the criterion. For the presented fractional-order controller tuning method the Nyquist criterion is automatically evaluated through Algorithm 1, which builds on Algorithm 2 and Algorithm 3. The method is here presented in a top-down approach. An illustration of the algorithm can be seen in Figure 1. Some details have been deliberately left out to avoid obfuscation of the main steps of the method. For details, see (Moltumyr, 2019a).

### *3.3 Fast Frequency Response Calculation*

Fast evaluation of stability properties is desirable when tuning controllers through optimization in the proposed way. This makes a fast and reliable evaluation of the frequency response of the open-loop transfer function a necessity. Naive approaches like linear or logarithmic fixed-step sampling, over some frequency interval, may easily fail to capture rapidly changing dynamics in parts of the response while oversampling other areas of the response. Leading to both loss of information and unnecessary calculations. Therefore, a method for fast calculation of the frequency response, built on the notion of adaptive stepping, has been developed. The method is presented in Algorithm 3.

**Algorithm 1** Automatic calculation of Nyquist Criterion

**Input:** $G(s)$, $C(s;\boldsymbol{x})$, $N_p$
**Output:** $\text{GM}_{\text{low}}$, $\text{GM}_{\text{high}}$

1: Find $L(s) = G(s)C(s;\boldsymbol{x})$ and calculate $L(j\omega)$ for $\omega \in [0,\infty]$ with Algorithm 3.
2: Make a list $\mathcal{P}$ of $\{\text{Re}\{L(j\omega_i)\},\omega_i\}$ and real-axis crossing direction (up or down) for all $\omega_i$ where $\text{Im}\{L(j\omega)\} == 0$. In case two proceeding values $\omega_i$ and $\omega_{i+1}$ satisfy $\text{sign}(\text{Im}\{L(j\omega_i)\}) \neq \text{sign}(\text{Im}\{L(j\omega_{i+1})\})$, use linear interpolation to estimate $\text{Re}\{L(j\omega_i)\}$ and $\omega_i$. $N$ is the length of list $\mathcal{P}$.
3: Divide the real axis from $-\infty$ to $\infty$ into $N+1$ segments $\mathcal{S}$ by cutting the real axis at the $N$ points in list $\mathcal{P}$.
4: Calculate $\mathcal{E}$, number of encirclements around each segment in $\mathcal{S}$, with Algorithm 2.
5: Using (11) where $N_n = 0$, if $e_i \in \mathcal{E}$ satisfies $e_i == N_p$ the system is stable when the corresponding segment $s_i \in \mathcal{S}$ contains the critical point $(-1,0)$. Add $s_i$ to a list $\mathcal{S}_{\text{stable}}$.
6: If $\mathcal{S}_{\text{stable}}$ is not empty, calculate and return lower and upper gain margins, $\text{GM}_{\text{low}}$ and $\text{GM}_{\text{high}}$ for all $s \in \mathcal{S}_{\text{stable}}$.

**Algorithm 2** Segment encirclement calculation

**Input:** $\mathcal{P}$, $N$
**Output:** $\mathcal{E}$

$\mathcal{E} = \text{zeros}(N+1)$
$A(1{:}2, 1{:}N) = \begin{bmatrix} \text{Re}\{L(j\omega_1)\} & \cdots & \text{Re}\{L(j\omega_N)\} \\ \omega_1 & \cdots & \omega_N \end{bmatrix}$
Sort $A$ w.r.t. 1st row
$A(3, 1{:}N) = 1{:}N$
Sort $A$ w.r.t. 2nd row
**for** $i = 1{:}N-1$ **do**
  $v = (A(3,i)+1){:}A(3,i+1)$
  **if** Length$(v) == 0$ **then**
    $v = (A(3,i+1)+1){:}A(3,i)$
  $dir = 1$ (up) or $-1$ (down)
  $d = \text{Re}\{L(j\omega_i)\} - \text{Re}\{L(j\omega_{i+1})\}$
  **if** $(dir == -1$ **and** $d > 0)$ **or**
    $(dir == 1$ **and** $d < 0)$ **then**
    $\mathcal{E}(v) = \mathcal{E}(v) - \text{ones}(\text{Length}(v))$
  **else if** $(dir == 1$ **and** $d > 0)$ **or**
    $(dir == -1$ **and** $d < 0)$ **then**
    $\mathcal{E}(v) = \mathcal{E}(v) + \text{ones}(\text{Length}(v))$

$L(s)$ is a fractional-order transfer function, with the same form as the right hand side of (4), whose frequency response is to be found. $\omega_{sp}$ is an input parameter that specifies the start point for the adaptive stepping. If the returned frequency response is not adequately continuous, $\omega_{sp}$ can usually be changed to improve continuity. The step-change constant $\beta > 1$ is a multiplicative factor used when changing step length $\omega_{sp}$. The stepping frequency $\omega_{\text{step}}$ is initialized with a low value in order for the algorithm to avoid taking too great steps at the start.

When calculating frequency response values at $\omega = 0$, all $b_l s^{\gamma_l}$ and $a_i s^{\eta_i}$ terms with $l > 0$ and $i > 0$ are dominated by the terms with $l = 0$ and $i = 0$. Similarly, for $\omega = \infty$, the terms with $l < m$ and $i < n$ are dominated by the terms with $l = m$ and $i = n$. Therefore,

$$\lim_{\omega\to 0} L(j\omega) = \frac{b_0}{a_0}\omega^{(\gamma_0-\eta_0)} e^{j\frac{\pi}{2}(\gamma_0-\eta_0)}\Big|_{\omega=0}, \tag{19}$$

$$\lim_{\omega\to \infty} L(j\omega) = \frac{b_m}{a_n}\omega^{(\gamma_m-\eta_n)} e^{j\frac{\pi}{2}(\gamma_m-\eta_n)}\Big|_{\omega=\infty}. \tag{20}$$

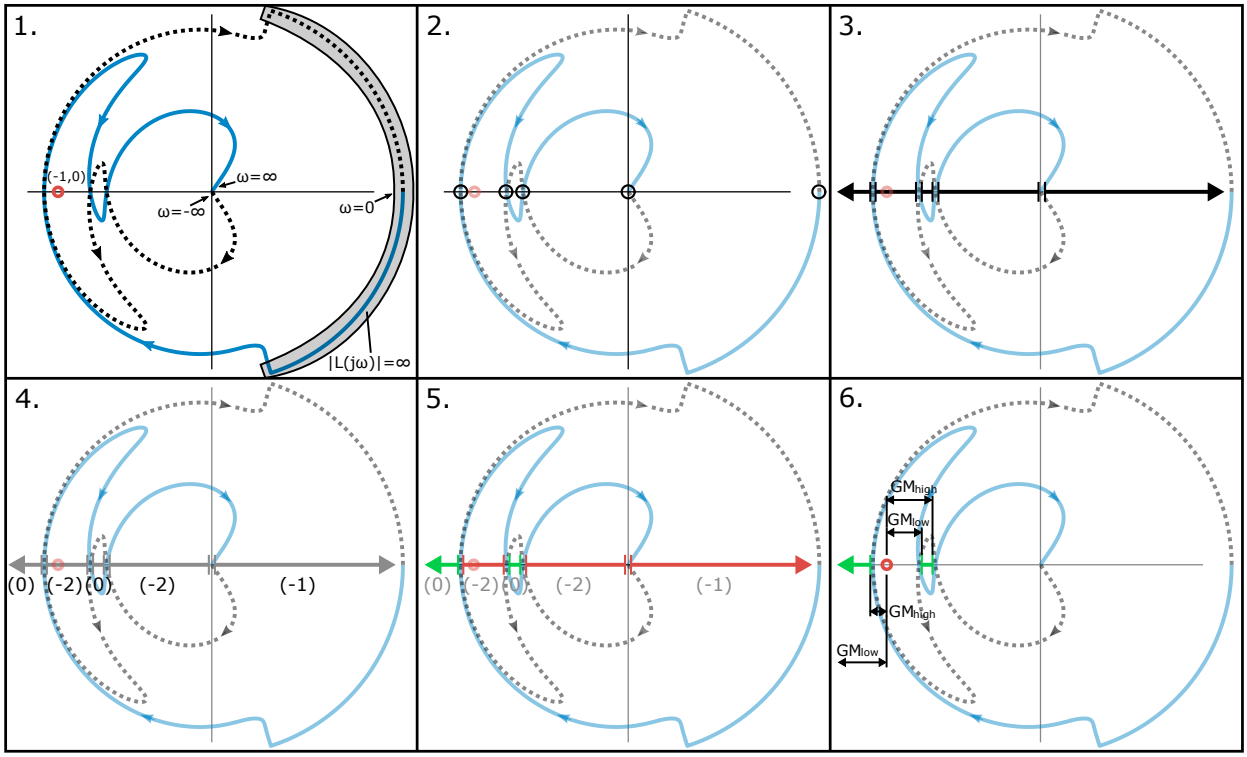


Fig. 1. Illustration showing the steps of the automatic calculation of Nyquist's stability criterion. The Nyquist curve is a logarithmic-polar plot of the fractional-order transfer function (25).

**Algorithm 3** Fast frequency response calculation

**Input:** $L(s)$ (FOTF object), $\omega_{sp}$, $\beta$
**Output:** $\{L(j\omega)$ for $\omega \in [0, \infty]\}$

1: Extract $b_l$, $a_i$, $\gamma_l$ and $\eta_i$ for $l = 1, 2, \ldots, m$ and $i = 1, 2, \ldots, n$ from FOTF object $L(s)$.
2: Calculate $\lim_{\omega\to 0} L(j\omega)$ and $\lim_{\omega\to\infty} L(j\omega)$ from (19) and (20), respectively.
3: Calculate $\{L(j\omega)$ for $\omega \in [\omega_{sp}, \infty\rangle\}$ according to flow diagram in Figure 2 and Equation (23) and (24) with positive $\omega_{\text{step}}$ value.
4: Calculate $\{L(j\omega)$ for $\omega \in \langle 0, \omega_{sp}]\}$ in the same way as in step 3, but with negative $\omega_{\text{step}}$ value.
5: Combine and return $\{L(j\omega)$ for $\omega \in [0, \infty]\}$.

Frequency response values can be calculated with

$$L(j\omega_k) = z_k = \frac{\sum_{l=0}^{m} b_l \omega_k^{\gamma_l} \left(\cos\left(\frac{\pi}{2}\gamma_l\right) + j\sin\left(\frac{\pi}{2}\gamma_l\right)\right)}{\sum_{i=0}^{n} a_i \omega_k^{\eta_i} \left(\cos\left(\frac{\pi}{2}\eta_i\right) + j\sin\left(\frac{\pi}{2}\eta_i\right)\right)}. \quad (21)$$

This is obtained by letting $s = j\omega_k$ in $L(s)$ and using Euler's formula

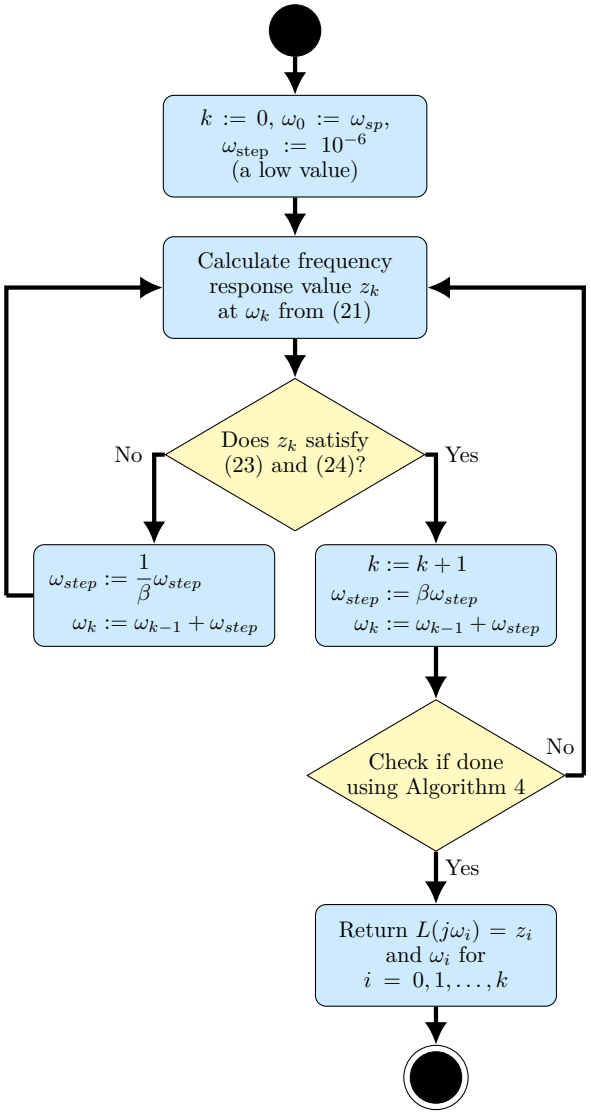


Fig. 2. Flow diagram showing the adaptive calculation of the frequency response in step 3-4 of Algorithm 3.

**Algorithm 4** Adaptive stepping end criterion

**Input:** $L(s = j\omega)$, $k$, $z_{k-1}$, $z_{k-2}$, $\omega_{step}$
**Output:** *done*

*done* = false
**if** $\omega_{step} > 0$ **then**
  $M = \lim_{\omega\to\infty} |L(j\omega)|$, $A = \lim_{\omega\to\infty} \arg(L(j\omega))$
  $R = \lim_{\omega\to\infty} \mathrm{Re}\{L(j\omega)\}$, $I = \lim_{\omega\to\infty} \mathrm{Im}\{L(j\omega)\}$
**else if** $\omega_{step} < 0$ **then**
  $M = \lim_{\omega\to 0} |L(j\omega)|$, $A = \lim_{\omega\to 0} \arg(L(j\omega))$
  $R = \lim_{\omega\to 0} \mathrm{Re}\{L(j\omega)\}$, $I = \lim_{\omega\to 0} \mathrm{Im}\{L(j\omega)\}$
$\Delta M = 0$
**if** $M == 0$ **or** $M == \infty$ **then**
  **if** $A - c_A \le \arg(z_{k-1}) \le A + c_A$ **then**
    $\Delta M = \Delta M + 20\left(\log_{10}|z_{k-1}| - \log_{10}|z_{k-2}|\right)$
    **if** $(M == \infty$ **and** $\Delta M \ge c_M)$ **or**
      $(M == 0$ **and** $\Delta M \le -c_M)$ **then**
      *done* = true
  **else**
    $\Delta M = 0$
**else**
  **if** $(|\mathrm{Re}\{z_{k-1}\} - R| < \delta_R$ **and** $|\mathrm{Im}\{z_{k-1}\} - I| < \delta_I$
    **and** $|\arg(z_{k-1}) - A| < \delta_A$ **then**
    *done* = true

$$j^\alpha = e^{j\frac{\pi}{2}\alpha} = \cos\left(\frac{\pi}{2}\alpha\right) + j\sin\left(\frac{\pi}{2}\alpha\right), \quad (22)$$

to calculate $j^\alpha$ for any power $\alpha \in \mathbb{R}$.

In order for the calculated frequency response to be sufficiently smooth, straight lines between the subsequent response values should not have a difference in slope of more than $c_1$. That is

$$|\arg(z_k - z_{k-1}) - \arg(z_{k-1} - z_{k-2})| < c_1. \quad (23)$$

In addition to the slope difference criterion, the change in magnitude between subsequent response values should not be too great with respect to the magnitude of the current response value. This is checked by assessing

$$\frac{|z_k - z_{k-1}|}{|z_k|} < c_2. \quad (24)$$

For the calculated frequency response to look smooth in a logarithmic Nyquist diagram and contain information of all real-axis crossings of $L(j\omega)$, which will be used later for assessing stability, $c_1$ and $c_2$ should not be chosen too big. On the other hand, the calculation of the frequency response should be fast in order for the repeated use of Nyquist criterion to be a feasible approach during optimization. So, $\omega_{step}$ should not be too small, which means that $c_1$ and $c_2$ should not be too big. Hence, a trade-off between precision and speed must be made when choosing these parameters. A value $c_1 = 5^\circ$ and $c_2 = 0.1$ were used in this work.

A dynamic end criterion described in Algorithm 4 was added to the frequency response calculation shown in Figure 2 in order to stop calculation when all the interesting dynamics have been captured. The end criterion detects and stops further calculations in two different ways depending on the values $\lim_{\omega\to 0} |L(j\omega)|$ and $\lim_{\omega\to\infty} |L(j\omega)|$ are 0 or $\infty$, or finite values between 0 and $\infty$:

(1) In case the magnitude at the limits are 0 or $\infty$, the end criterion stops further calculations if $\arg(L(j\omega))$ has

stayed sufficiently close to $\arg(L(j\infty))$ or $\arg(L(j0))$ while $|L(j\omega)|$ has increased or decreased towards $|L(j\infty)|$ or $|L(j0)|$ with a total sum of $c_M$ decibel. With 'sufficiently close', we here mean an interval of $c_A$ degrees on either side of $\arg(L(j\infty))$ or $\arg(L(j0))$.

(2) In case a limit magnitude value is finite, the end criterion stops further calculations if $L(j\omega_i)$ is sufficiently close to the finite value at the limit. What is considered 'sufficiently close' is determined by parameters $\delta_R$, $\delta_I$ and $\delta_A$.

Table 1. Parameters used in Algorithm 4: adaptive stepping criterion.

| $c_A$ | $c_M$ | $\delta_R$ | $\delta_I$ | $\delta_A$ |
|---|---|---|---|---|
| 5° | 30 dB | $10^{-6}$ | $10^{-6}$ | 0.1° |

The frequency response calculation method in Algorithm 3 may stop early for some systems because of the way the end criterion in Algorithm 4 is formulated. Algorithm 4 checks the frequency response for a phase-magnitude pattern that is consistent with the phase and magnitude values at $\omega = 0$ and $\omega = \infty$. For some systems this phase-magnitude pattern may be detected at some earlier point, terminating the calculation too early. The likelihood of this happening depends on the specific system and the parameter $c_M$. In the event that this should happen, increasing $c_M$ should stop early termination at the cost of an increase in computation time.

Stability calculation with Algorithm 1 may therefore be incorrect if one or more points where $\mathrm{Im}(L(j\omega)) = 0$ has been dropped, or the linear interpolation approximation done in Algorithm 1 to find points on the real axis is not precise enough because the neighbouring points are too far apart. Therefore, no guarantee for correctness can be given for the method.

## 4. FRACTIONAL-ORDER LOGARITHMIC NYQUIST DIAGRAM

To visualize the stability of fractional-order systems expressed in Laplace-domain and to support the stability calculations in the proposed tuning method, a logarithmic Nyquist diagram supporting fractional-order systems was developed. With this diagram and the knowledge about the number of fractional unstable poles in the open-loop fractional system, the stability of the closed-loop fractional-order system can be established. The advantage of this diagram over a regular Nyquist diagram is that no zooming is necessary to get a good understanding of how many times the graph circles around the critical $z = -1 + j0$ point. The inspiration for the diagram comes from Andresen (2001), which presents the diagram for integer order systems, under the name "Logarithmic-Amplitude Polar diagram".

*Example 1.* A logarithmic Nyquist diagram of the fractional-order transfer function

$$L_1(s) = \frac{200(1+3s)(1+2s)}{s^{0.8}(1+22s^{1.3}+(22s^{1.3})^2)(10+s)(20+s)}, \quad (25)$$

is shown in Figure 3. The critical $-1 + j0$ point is shown as a black circle. Counting encirclements around $-1 + j0$

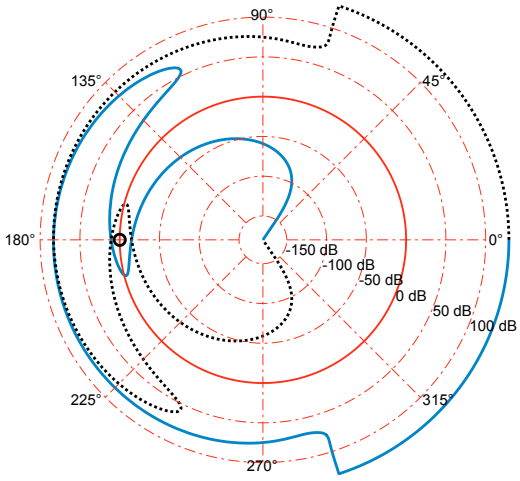


Fig. 3. Logarithmic Nyquist Diagram of $L_1(s)$, represented as a FOTF object, plotted with Matlab.

we see that the Nyquist curve does not encircle this point ($\angle(1+L(j\omega)) = 0$). Knowing that $L(s)$ is open-loop stable ($N_p = 0$), in addition to the number of encirclements, we conclude that $N_n$ must be equal to zero, which tells us that the closed-loop system will also be stable.

## 5. SIMULATION RESULTS

To demonstrate the usefulness of the proposed tuning method, an example showing the results from tuning a regular PID and a fractional-order PID controller with this method to an identified integer-order plant model of a nanopositioning stage along the lateral axes in an atomic force microscope (AFM) is presented (Moltumyr, 2019b). The nanopositioning model is open-loop stable and the controller parameters $\boldsymbol{x}$ are bounded by $\boldsymbol{x}_{lower}$ and $\boldsymbol{x}_{upper}$ to ensure open-loop controller stability. Therefore $N_p = 0$ and $\Delta\angle(1 + L(j\omega))$ should equal zero for the closed-loop system to be stable. The controllers have the following structure, where $x_i$ are the controller parameters to be optimized,

$$C_{PID}(s) = x_1 + \frac{x_2}{s} + \frac{x_3 s}{1 + x_4 s}, \quad (26)$$

$$C_{FO-PID}(s) = x_1 + \frac{x_2}{s^{x_5}} + \frac{x_3 s^{x_6}}{1 + x_4 s^{x_6}}. \quad (27)$$

Simulation results from the tuning can be seen in Figure 4, 5 and 6. Controller parameters can be found in Table 2. The identified AFM model $G(s)$ is of 15th order and has relative degree one. Due to the size of $G(s)$ the transfer function is not given here. However, the frequency response of $G(s)$ can be seen in Figure 5, together with the PID and FO-PID controlled closed-loop responses $T_{PID}(s)$ and $T_{FO-PID}(s)$. From Figure 6 we observe that $\Delta\angle(1 + L(j\omega)) = 0$ for both the controllers and conclude that both the systems are stable. Which is supported by the step response plots in Figure 4.

A minimum gain margin of $\Delta k = 6\,\mathrm{dB}$ was used during the controller parameter optimizations. When complete, both of the systems did show a gain margin of about 6 dB. Adding different open-loop gains around 6 dB to the systems and simulating with Simulink and the FOTF

Table 2. Controller parameters for controller (26) and (27) found with the proposed tuning method.

| Type | $x_1$ | $x_2$ | $x_3$ | $x_4$ | $x_5$ | $x_6$ |
|---|---|---|---|---|---|---|
| PID | $1.98 \cdot 10^{-2}$ | $3.89 \cdot 10^{3}$ | $7.04 \cdot 10^{-2}$ | 1.48 | 1 | 1 |
| FO-PID | 1.37 | $1.07 \cdot 10^{5}$ | $1.57 \cdot 10^{1}$ | $1.00 \cdot 10^{2}$ | 1.419 | 1.367 |

toolbox shows a good correspondence between when the step responses show stable behavior and when the systems are stable according to Nyquist's criterion.

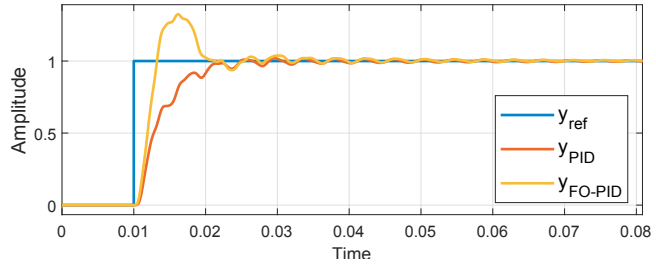


Fig. 4. Closed-loop step response of AFM model with two different controllers. Simulated with Simulink and the FOTF toolbox (Xue, 2017).

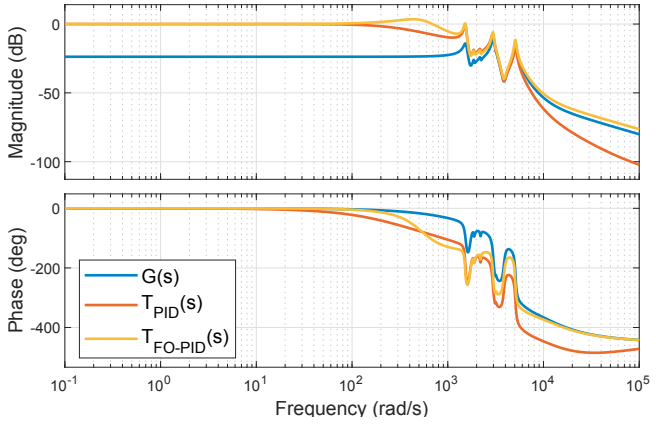


Fig. 5. Bode diagram of the AFM model with two different controllers.

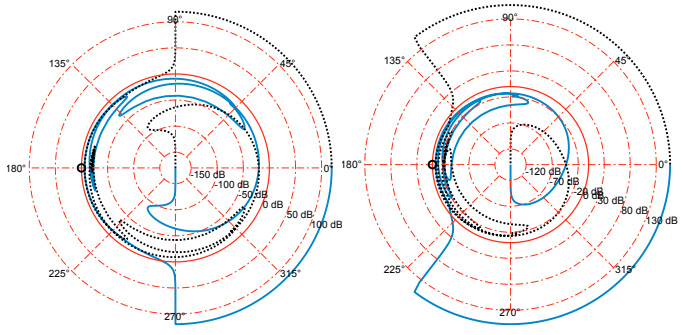

(a) PID (b) FO-PID

Fig. 6. Logarithmic amplitude polar diagrams of the AFM model with two different controllers.

## 6. DISCUSSION

Although the proposed optimization tuning method manages to find stable solutions, the optimal solution in terms of the presented objectivity function and optimization method does not give satisfactory results when looking at the step responses in Figure 4. From the step response, we see that the tuned fractional-order PID controller has a significant peak as opposed to the regular PID controller. This is likely a result of not including time-domain information into the objectivity function (15).

Adding a time-domain objective to (15) like the integral of squared error (ISE) of the difference between step and step response was considered. However, making a normalized measure of the step-response error that could handle variable time frames, had a reliable and stable simulation method and where the step response shape could be easily compared from iteration to iteration, while still being fast to evaluate, proved somewhat challenging. Hence, no further attempt was made at adding a time-domain objective to (15, and is, therefore, a topic for further work.

Only simultaneous tuning of all controller parameters was attempted in this work. Presetting some of the parameters while tuning others could help reduce the search space and improve on the results. Besides, tuning of the filter coefficient $x_4$ is most likely unnecessary since the filter's main purpose is to make the controller transfer function proper. Testing different controllers and selective tuning of parameters are therefore areas of further inquiry.

In this work, the genetic algorithm was chosen for non-linear optimization early on because of the GAs good ability to escape local minima. However, no in-depth study or comparison of different non-linear optimization methods were made. Therefore, it cannot be concluded whether GA is the best approach in this case or if there exist other more suitable methods.

## 7. CONCLUSION

A heuristic optimization-based method using the genetic algorithm and Nyquist's stability criterion for controller tuning supporting arbitrary integer-order and fractional-order systems have been presented. Controller tuning with the proposed method and simulation results with Matlab and Simulink shows the validity of the method. Also, the use of logarithmic Nyquist diagrams for visualizing closed-loop stability of fractional-order systems have been proposed.

## REFERENCES

Altintas, G. and Aydin, Y. (2017). Optimization of fractional and integer order PID parameters using big bang big crunch and genetic algorithms for a MAGLEV system. In *20th IFAC World Congress*, 4881–4886. Toulouse, France.

Andresen, T. (2001). A logarithmic-amplitude polar diagram. *Modeling, Ident. and Control*, 22(2), 65–72.

Dabiri, A., Moghaddam, B.P., and Machado, J.A.T. (2018). Optimal variable-order fractional PID controllers for dynamical systems. *Journal of Computational and Applied Mathematics*, 339, 40–48.

Dastjerdi, A.A., Saikumar, N., and HosseinNia, S.H. (2018). Tuning guidelines for fractional order PID controllers: Rules of thumb. *Mechatronics*, 56, 26–36.

David, S., López, J., and Pallone, E. (2011). Fractional order calculus: Historical apologia, basic concepts and some applications. *Revista Brasileira de Ensino de Física*, 33.

Dorćák, L., Petráš, I., Koštial, I., and Terpák, J. (2002). Fractional-order state space models. In *3rd International Carpathian Control Conference (ICCC)*, 193–198. Malenovice, Czech Republic.

Eielsen, A.A., Vagia, M., Gravdahl, J.T., and Pettersen, K.Y. (2014). Damping and tracking control schemes for nanopositioning. *IEEE/ASME Transactions on Mechatronics*, 19(2), 432–444.

Guefrachi, A., Najar, S., Amairi, M., and Aoun, M. (2017). Tuning of fractional complex order PID controller. In *20th IFAC World Congress*. Toulouse, France.

Holland, J. (1992). *Adaptation in natural and artificial systems: an introductory analysis with applications to biology, control, and artificial intelligence*. MIT Press, Cambridge, USA.

Kumar, L., Kumar, P., Satyajeet, and Narang, D. (2018). Tuning of fractional order $PI^{\lambda}D^{\mu}$ controllers using evolutionary optimization for PID tuned synchronous generator excitation system. 859–864.

Mandić, P.D., Šekara, T.B., Lazarević, M.P., and Bošković, M. (2017). Dominant pole placement with fractional order PID controllers: D-decomposition approach. *ISA Transactions*, 67, 76–86.

MathWorks (2019). Matlab global optimization toolbox user's guide. URL `https://www.mathworks.com/help/pdf_doc/gads/gads_tb.pdf`. (Accessed: 2019-03-21).

Matignon, D. (1996). Stability results for fractional differential equations with applications to control processing. In *Computational Engineering in systems applications. Proc. of IMACS-SMC*, volume 2, 963–968. Lille, France.

Moltumyr, A.H. (2019a). Focs_nyqopt_design v0.1-beta, github. URL `github.com/mltmyr/FOCS_NyqOpt_design`. (Accessed: 2019-11-05).

Moltumyr, A.H. (2019b). *Control in Atomic Force Microscopy: A Fractional Order Approach*. Master's thesis, Norwegian U. of Science and Technology, Trondheim, Norway.

Nyquist, H. (1932). Regeneration theory. *The Bell System Technical Journal*, 11(1), 126–147.

Oustaloup, A., Levron, F., Mathieu, B., and Nanot, F.M. (2000). Frequency-band complex noninteger differentiator: characterization and synthesis. *IEEE Trans. on Circuits and Systems I: Fund. Theory and Appl.*, 47(1), 25–39.

Podlubny, I. (1999). *Fractional differential equations : an introduction to fractional derivatives, fractional differential equations, to methods of their solution and some of their applications*, volume 198 of *Mathematics in science and engineering*. Academic Press, San Diego, CA.

Sabatier, J., Farges, C., and Trigeassou, J.C. (2013). A stability test for non-commensurate fractional order systems. *Systems & Control Letters*, 62(9), 739–746.

Skogestad, S. and Postlethwaite, I. (2001). *Multivariable feedback control: Analysis and design*. Wiley, New York, USA, 2 edition.

Sun, G., Wu, L., Kuang, Z., Ma, Z., and Liu, J. (2018). Practical tracking control of linear motor via fractional-order sliding mode. 94, 221–235.

Trächtler, A. (2016). On BIBO stability of systems with irrational transfer function. *arXiv:1603.01059 [math.DS]*.

Trigeassou, J.C. and Maamri, N. (2009). A new approach to the stability of linear fractional systems. In *6th Int. Multi-Conf. on Systems, Signals and Devices*, 1–14. Djerba, Tunisia.

Xue, D. (2017). *Fractional-order control systems: Fundamentals and numerical implementations*. Fractional calculus in applied sciences and engineering 1. De Gruyter, Berlin, Germany.

Zhou, J. (2017). A nyquist-like approach for stability analysis in fractional-order systems: Related issues and case studies. In *2017 29th Chinese Control And Decision Conference (CCDC)*, 999–1003. Chongqing, China.